Materials Transactions, Vol. 47, No. 7 (2006) pp. 1717 to 1722
Special Issue on Thermal Spraying

Preparation and Evaluation of Ordinary Attritor Milled Ti-Al Powders and Corresponding Thermal Sprayed Coatings

Masahiro Fukumoto, Min Nie* and Toshiaki Yasui

Department of Production Systems Engineering, Toyohashi University of Technology, Toyohashi 441-8580, Japan

Ordinary attritor milling of elemental metallic powders under atmospheric condition was utilized to prepare desirable amount of powders for thermal spraying. The effect of different BPR (Ball to Powder weight Ratio) has been investigated in terms of nitridation during milling. To investigate the effect of heat treatment on the formation of dispersed phases, heat treatment to the powder was performed as well. Titanium aluminide coatings with carbonitride dispersed phases were successfully fabricated by low pressure plasma spraying. The hardness and specific wear of the coatings prepared by the powders with different milling conditions was measured so as to investigate the effect of the content of dispersed titanium based carbonitride phases. Experimental results show that the formation of dispersed carbonitride phases depends strongly on milling condition, irrespective of heat treated powders or thermal sprayed coatings, and directly affects the mechanical properties of the coatings. Compared with the phase composition of heated powders and corresponding thermal sprayed coatings, it seems that the temperature of processing the MA powders is also a decisive factor on the phase formation, especially carbonitride phases and oxide phase.
[doi:10.2320/matertrans.47.1717]

(Received November 21, 2005; Accepted June 1, 2006; Published July 15, 2006)

Keywords: *ordinary attritor mill, milling condition, titanium based carbonitride, heat treatment, low pressure plasma spraying, TiAl coating, hardness, specific wear*

1. Introduction

Intermetallic compounds have aroused great interest during the last decade due to their attractive properties for potential high temperature applications. In particular, titanium aluminides, which are blessed with exceptional combination of properties such as low density, high corrosion and oxidation resistance, and high temperature strength, are promising candidates for structural components in high-speed aircraft and reusable launch vehicles. However, the Achilles' heel of these intermetallics-poor room temperature (RT) ductility and toughness has prevented the widespread application of these materials. In order to improve or overcome their RT ductility, a lot of approaches have been tried. Among these, aggressively, extreme grain size refinement by mechanical alloying (MA)[1–3] is one of the most practical processing philosophies. Moreover, as is well known, to prepare intermetallics as coatings is one of the best ways to avoid the workability problem, which is caused by RT ductility, encountered in the conventional rolling process.

A lot of investigation has been carried out in terms of MA of powder mixtures of pure titanium and aluminum.[4–11] The effect of the milling parameters such as milling tools, different milling atmosphere, different combination of powders and the addition of different process control agent (PCA's), was widely investigated. Most of the results show that amorphization should be accomplished after long time milling under Ar atmosphere, which is in good accordance with the theoretical calculation.[5] However, some researchers reported that a phase with fcc structure (TiN) might be formed while the milling was conducted under Ar atmosphere, due to the ineffective seal of the milling tools.[6–9] Additionally, TiC (fcc structure) was also obtained due to the decomposition of PCA's during mechanochemical synthesis of elemental Ti and Al powder mixture.[10,11] It is obvious now that nitride and carbide contamination phases are easily formed due to the inherent nature of Ti as a reactive metal.[2] It is worth mentioning that most milling equipments like shaker milling, planetary ball milling and tumbler ball milling, used by those researches were not acceptable for industrial applications due to the limitation of the total powder yield. Instead, the ordinary attritor milling, a simple, yet efficient, and scalable way, is capable to provide more feedstock for wider or deeper researches and applications.

On the other hand, thermal spraying offers a novel and economical method of fabricating titanium aluminide coatings. During thermal spraying, the powder particles are heated, and the molten and half molten particles are accelerated, striking the substrate, deformed to lamellae, and building up a coating eventually. Low pressure plasma spraying (LPPS) is a promising way for excluding the disturbances of the atmosphere during thermal spraying.[12] Inside the chamber filled with low pressure inert gas, dense, adherent and homogeneous coating can be easily formed. Attempts have been tried to disperse the nitride particles to titanium aluminide to improve its mechanical property. Yuki *et al.*[13] investigated the casting of γ titanium aluminide alloys under N_2 atmosphere. The precipitates of nitride were found to be effective in refining the $TiAl/Ti_3Al$ lamellar grains. Tsunekawa *et al.*[14] prepared the titanium aluminide matrix *in situ* composite coatings by reactive low pressure plasma spraying (RLPPS). Nitrogen plasma was applied in this reaction synthesis process, which resulted in the formation of the *in situ* reinforcement. Moreover, Hoshiyama *et al.*[15] has reported that nitride and carbide dispersed composite coatings were fabricated by LPPS using Ar/H_2 plasma. The powder feedstock was prepared by ball milling of elemental titanium and aluminum powders under nitrogen atmosphere. However, only limited information was provided about ball milled powders and the effect of milling condition on the final nitride phase formation of the coatings.

The objective of the present research is to investigate the nitridation progress of the powder mixture of elemental

*Graduate Student, Toyohashi University of Technology titanium and aluminum powders milled by ordinary attrior under atmospheric condition, and the effect of the milling conditions on the final nitride phase formation of the coatings fabricated by LPPS. In addition, the heat treated attritor milled powders were also studied so as to investigate the temperature effect on final phase formation.

2. Experimental Procedures

Elemental powders of Ti (>99.9%, <45 µm) and Al (>99%, <150 µm) in the atomic ratio of 50:50 were used as starting materials. With the same amount of milling media (SUJ2 balls, 9.6 mm in diameter, 12 kg) and PCA'S (methanol, 10 g), attritor milling was conducted under atmospheric condition, respectively, for three batches of powders of different weight of starting materials in various milling time, namely, SM 100 (BPR (Ball to Powder weight Ratio), 120:1), SM 200(BPR, 60:1) and SM 300(BPR, 40:1).

Heat treatment of as prepared powders was performed using the same heating condition. Under flowing argon atmosphere, as prepared powders were annealed for 10 min at 1200°C.

After sieving, as prepared powders with particle size less than 53 µm were employed as spraying feedstock. The chamber of LPPS system was evacuated to a pressure less than 0.5 kPa before spraying. The coatings were fabricated onto grit blasted Ti-6Al-4V substrate using the following parameters: primary gas, Ar: 50 L/min, secondary gas, He: 10 L/min, power: 19.2 kW, pressure during spraying: 13.3 kPa, spraying distance: 200 mm, preheating time: about 10 sec, spraying time: 3 min. After spraying, the substrate was naturally cooled down to room temperature inside the chamber filled with inert gas.

The phase compositions of powders and coatings were determined by X-ray diffraction (XRD) using Cu Kα radiation. The relative intensity ratio of phase (relative amounts of the phase) was evaluated according to XRD data using the following method: The relative intensity ratio of the phase is equal to the peak intensity of that phase (main peak) divided by the sum of peak intensity (main peak only) of all the phases appeared in the same XRD pattern. The microstructure of the powders and coatings was characterized by scanning electron microscopy. Transmission electron microscopy was occasionally used for precise identification of grain size and phases with respect to as prepared powders. The microhardness of the cross section of the coatings was measured by a Shimadzu HMV-2 Micro-Hardness Tester. Hardness test for each coating was performed 12 times using a load of 100 g to ensure obtaining a reasonably average value. An Ohkoshi type wear machine was used to evaluate the wear resistance of coatings. Wear testing conditions were friction distance: 200 m, friction velocity: 1.97/s, final load: 63 N.

3. Results and Discussions

3.1 Characterization of milled powder

Figure 1 shows the XRD pattern of each powder (SM 200) milled by ordinary attritor for various hours. With increasing milling time, the XRD peaks exhibit broadening and peak intensity decreasing, which caused by refinement of crystalline size and development of lattice strain resulted from the significant disordering during mechanical alloying. However, the diffraction peak at $2\theta \approx 35°$ (Ti(100)), which was supposed to be following the peak intensity decreasing tendency of another two Ti peaks (Ti(002) ($2\theta \approx 38°$), Ti(101) ($2\theta \approx 40°$)) if the Ti(Al) solid solution were exclusively formed, remains relatively intense. Therefore, the intense peak at $2\theta \approx 35°$ is not due to either elemental phase. Keskinen *et al.*[11] reported the presence of $TiH_{1.924}$ and TiC phase in Ti-Al powder mixtures mechanically alloyed with organic PCA's. The traces of these two phases are observable in accordance with the XRD patterns of as milled powders (Fig. 1). On the other hand, the expected peaks for TiN phase, whose positions are indicated by dot line in the figure, became more evident with increasing milling time. According to the JCPDS data,[16] the coexistence of $TiH_{1.924}$, TiC and TiN with Ti makes it difficult to verify each phase in XRD pattern. Presumably, metastable phases-$TiH_{1.924}$ and Ti(N, C) were gradually formed, due to the decomposition of the PCA's (methanol) and aggressive involvement of the atmosphere (N_2) in the course of mechanical alloying.

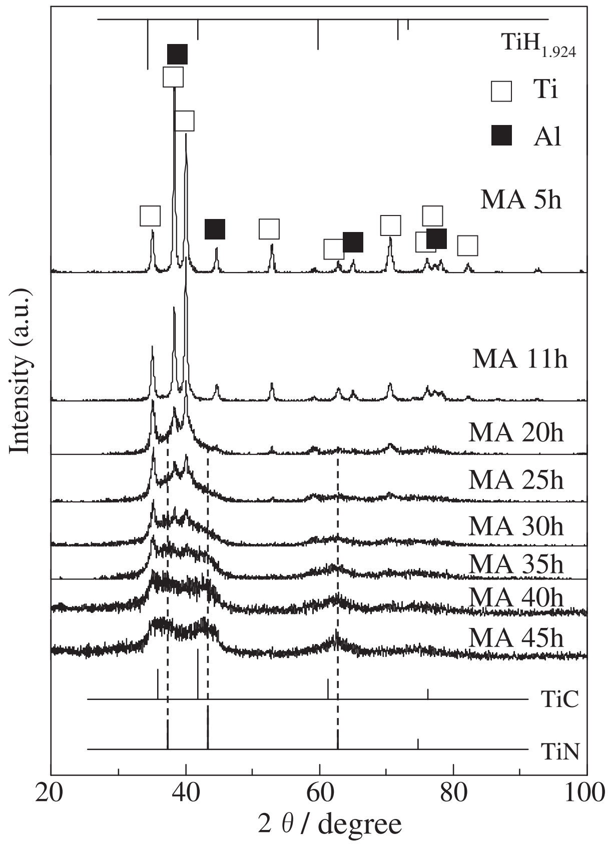

Fig. 1 Change in the X-ray diffraction pattern of Ti-Al powder mixture (SM 200) with the progress of milling.

XRD patterns of MA 25 h powders milled with different BPR-120:1 (SM 100), 60:1 (SM 200) and 40:1 (SM 300), are shown in Fig. 2. In the case of SM 100, it is obvious that a phase with fcc structure was formed. Further evidence can be provided by its TEM observation results as shown in Fig. 3. Along with fine grains (<10 nm), the fcc structure was

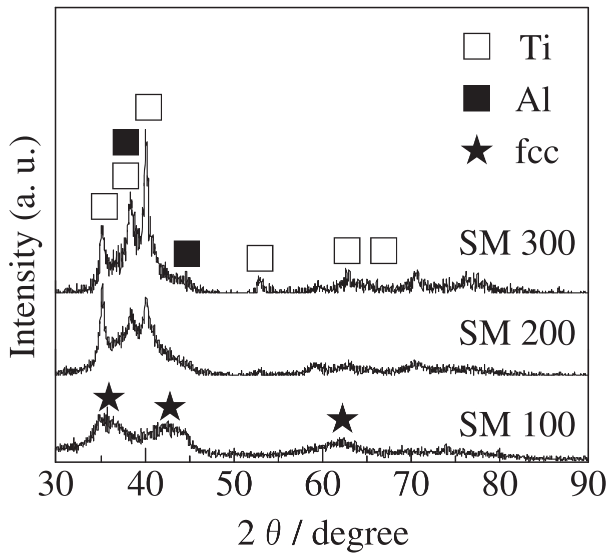

Fig. 2 XRD patterns of MA 25 h powders prepared with different BPR–120/1 (SM 100), 60/1 (SM 200) and 40/1 (SM 300), respectively.

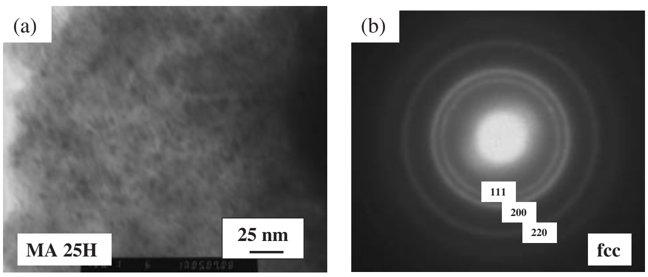

Fig. 3 TEM micrographs of frequently observed regions of MA 25 h powders (SM 100): (a) Bright field image; (b) Associated electron diffraction pattern.

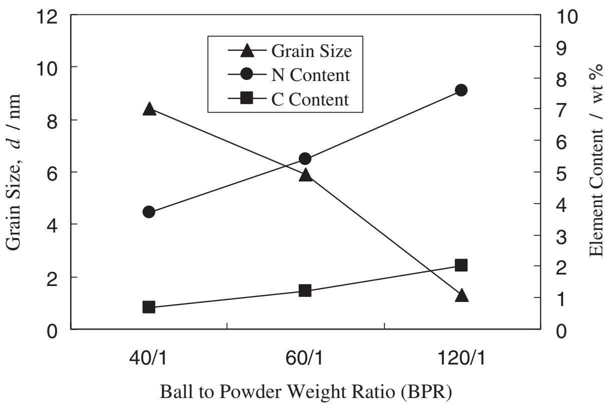

Fig. 4 Relation between grain size of MA 25 h powders milled using different BPR and the corresponding content of light elements (N, C).

distinctively present according to the associated electron diffraction pattern of MA 25 h powders (SM 100).

Figure 4 illustrates the relation between content of light elements (N, C) as measured through chemical analysis and the average grain size of MA 25 h powders milled with different BPR as estimated by Scherrer's equation. As is well known, X-ray peak broadening method-Scherrer's equation

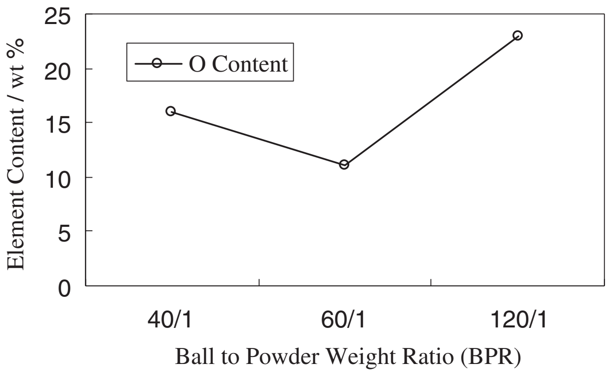

Fig. 5 The O content of MA 25 h powders versus the BPR.

is acceptable if only interested in the trend of change of grain size with milling condition.[2] With increasing BPR, the average grain size of corresponding powders decreases, while the N and C content of corresponding powders increases. It is concluded that higher milling energy (higher BPR) would result in higher efficiency in terms of grain size refinement. Consequently, higher content of picked up N and C element could be achieved because of the availability of new fresh faces with larger surface area.

It is worth noting the O content of the as milled powders. As shown in Fig. 5, MA 25 h powders, irrespective of the BPR used, show high O content, although no oxide phase was identified according to their associated XRD pattern. Taking into account of contamination from Oxygen and the powder yield of the as milled powders, only SM 200 powder batch (up to MA 25 h) was prepared for feedstock of LPPS spraying. As for comparison, the heat treatment of SM 200 powder batch was conducted as well.

3.2 Effect of heat treatment to the powder

XRD patterns of heat treated powders (SM 200) are shown in Fig. 6. In the case of heat treated MA 5 h powders, the main phases are γ (AlTi) and α_2 ($AlTi_3$), but the traces of $Ti_2Al(N, C)$ and Al_2O_3 are evident. With increasing MA time, $Ti_2Al(N, C)$ phase gradually becomes a prominent and becomes the exclusively main phase in the case of MA 30 h powders.

An intuitive illustration of the phase evolvement of the heat treated powders with respect to milling time is shown in Fig. 7. With increasing MA time, the relative intensity ratio of γ and α_2 gradually decreases, while that of $Ti_2Al(N, C)$ increasing significantly and that of Al_2O_3 increasing slightly. It is worth mentioning that α_2 is absent since MA 20 h after heat treatment. As is well known, the composition of Ti-Al (50:50 in atomic ratio) is the dual phase region containing γ and α_2. The single γ region is located in 51–56 pct Al. Therefore, after heat treatment, it is prone to form γ rather than α_2 with increasing MA time because of the higher homogeneity of the mixed powders. Moreover, the formation of $Ti_2Al(N, C)$ might precede the formation of α_2 during annealing. Wang[17] has reported that the formation of Ti_2AlN preceded the formation of α_2 for the Ti-Al matrix containing N atoms during the heating process. In addition, it should be pointed out that the formation of Al_2O_3, which can be

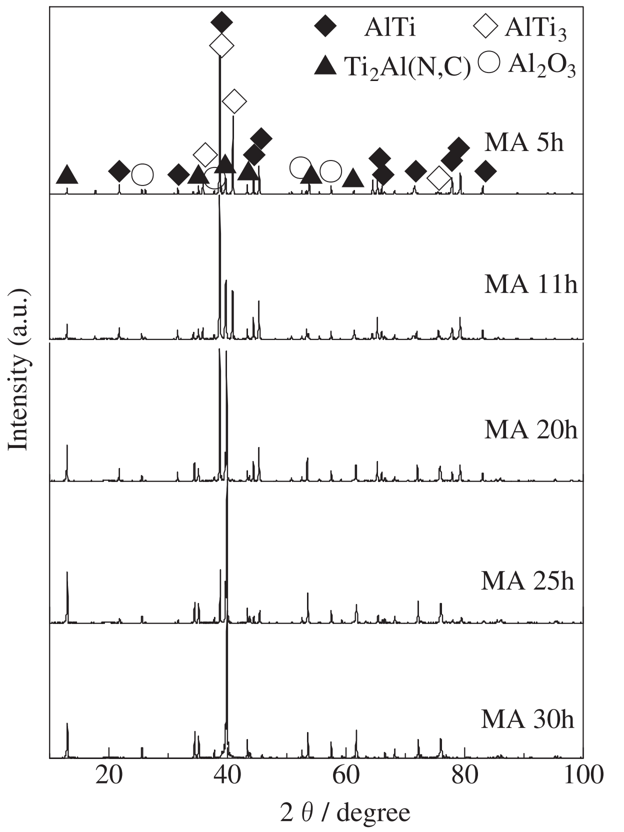

Fig. 6 XRD patterns of heat treated attritor milled Ti-Al powders (SM 200) of different milling time.

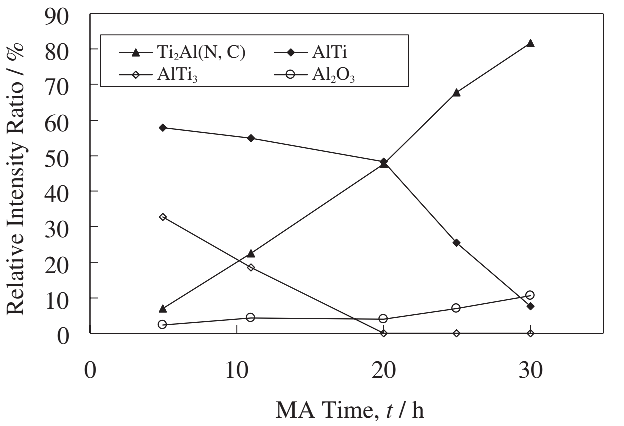

Fig. 7 Relative intensity ratio of each phase in heat treated powders with increasing milling time.

traceable to the picked up O content in the course of mechanical alloying, might contribute to the complexity of the reaction mechanism of the heat treated powders.

Figure 8 shows the typical SEM images of the cross section of heat treated MA 20 h powders (SM 200). As shown in Fig. 8(b), it is evident that fine dark particles homogeneously distributed in the powder matrix. In accordance with its associated XRD pattern, those dark particles are presumably Ti_2Al(N, C) phase. However, due to the presence of small scales of Al_2O_3 along with the existence of porosities in the heat treated powders, the identification of the dark phase might be kind of subjective.

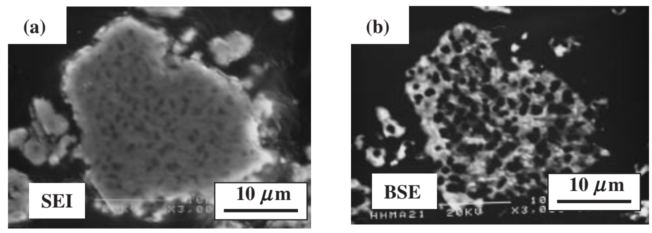

Fig. 8 Typical SEM images of the cross section of heat treated MA 20 h powders (SM 200): (a) SEI image; (b) Corresponding BSE image.

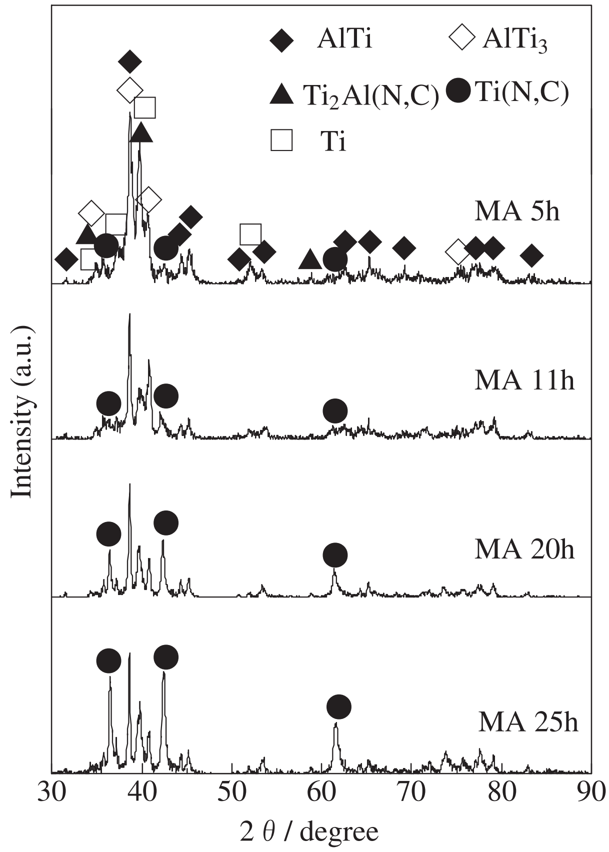

Fig. 9 XRD Patterns of coatings fabricated by LPPS using SM 200 powder batch.

3.3 Thermal sprayed coatings

3.3.1 Microstructure of coatings

XRD patterns of thermal sprayed coatings prepared by attritor milled SM 200 powder are illustrated in Fig. 9. In addition to the formation of Ti_2Al(N, C) phase, the trace of another kind of titanium based carbonitride phase-Ti(N, C) was observable and it became gradually prominent with increasing milling time. Moreover, a certain fraction of Ti phase was present in the coatings, especially in the MA 5 h and MA 11 h coatings, and oxide phase was surprisingly absent in all the fabricated coatings. Compared with the heat treatment conducted in the present study, thermal spraying process is a totally different thermal process with respect to the temperature distribution of the heat source and heating condition of the powders. Whereas the measurement of the velocity and temperature to the particles was not conducted in the present study, the velocity of the flying particles may

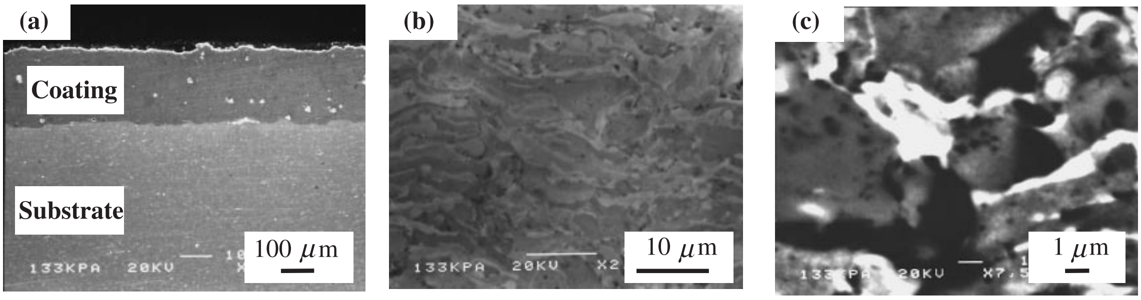

Fig. 10 Typical SEM micrographs of the cross section of MA 20 h coating: (a) General view (SEI); (b) Low magnification (SEI); (c) High magnification (BSE).

range between a few tens of ms^{-1} and about 400–500 ms^{-1} for particles fully or partially melted at impact, and the temperature of the flying particles varies from 1000 to 4500°C, as reported in the references.[18] Thus, the mechanism of phase formation in thermal sprayed coatings is quite different from that in the heat treated powders. Considering the higher velocity of the sprayed particles and the boiling point of Ti (3259°C) and Al (2520°C), the higher possibility of evaporation of Al during the flight of powder particle might reduce the opportunity of reaction between Ti and Al elements, especially for as milled powders in the early stage of mechanical alloying (MA 5 h, MA 11 h), which resulted in the higher content of Ti phase in those coatings. On the contrary, the higher possibility of evaporation of Al might facilitate the reaction between Ti and light elements (C, N) under high temperature, which leaded to the formation of Ti (N, C) phase.

The typical SEM observation results on the cross section of MA 20 h coating are shown in Fig. 10. Under low magnification, as shown in Fig. 10(b), the coating shows typical lamella structure associated with thermal spraying. The dark colored lamella is mainly composed of γ phase, while the light colored lamella is mainly composed of α_2 phase, in accordance with XRD pattern of the coating. Under high magnification, as shown in Fig. 10(c), presumably, the precipitated dark, titanium based carbonitride phases, can be observed in the intermetallic matrix. Due to the coexistence of micro-porosities, which appear in dark color in SEM image, especially BSE, distinguishing the precipitated hard phases from the micro-porosities is difficult.

3.3.2 Mechanical properties of coatings

In the present study, the highest value (average value) of Vickers microhardness of the coating cross section is 810 Hv (MA 20 h coating), which was achieved by increasing the milling time of spraying feedstock to 20 h. The hardness of γ TiAl casting is about 250 Hv (Maximum),[19] and 550 Hv (Maximum) for nitride dispersed sintered TiAl bulk.[13] Hoshiyama *et al.*[15] prepared Ti-Al-N composite powder by ball milling of elemental titanium and aluminum for about 84 h under nitrogen atmosphere, and the maximum value of microhardness of corresponding coating fabricated by LPPS is about 600 Hv as reported in their paper. On the other hand, Tsunekawa *et al.*[14] utilized RLPPS to fabricate nitride dispersed TiAl coating using premixed Ti/Al powder, and coating with improved hardness of about 700 Hv was fabricated by addition of Mn and Nb to the premixed powders and activation of the nitride formation by means of transferred arc. Although the indentation load is different, for example, 25 g in Ref. 13), the hardness obtained in the present research is fairly higher than the others. It indicates that the hardness of coating can be effectively improved by simply controlling the milling time of attritor milled elemental Ti and Al powder mixture. Figure 11 illustrates the relation between microhardness of the coatings prepared by attritor milled SM 200 powder and the relative intensity ratio of Ti(N, C) in each coating. The microhardness of thermal sprayed coatings is much higher than Ti alloy substrate (Ti-6Al-4V). Generally speaking, the relative intensity ratio of Ti(N, C) increases as a function of MA time and the microhardness of the corresponding coating seems to increase as a result. It should be pointed out that only little difference between the microhardness of MA 20 h coating and that of MA 25 h coating was presumably caused by the microporosities.

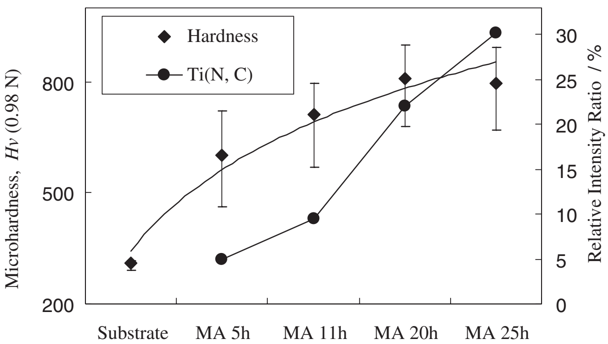

Fig. 11 Relation between microhardness of coatings prepared by attritor milled SM 200 powder batch and the relative intensity ratio of Ti(N, C) phase in each coating. (Note: Hardness test results of substrate (Ti-6Al-4V) is included in the figure)

Finally, the relation between specific wear of the coatings prepared by attritor milled SM 200 powder and the relative intensity ratio of Ti(N, C) in each coating is shown in Fig. 12. As for comparison, wear testing of Ti alloy substrate was conducted using the same testing condition. Its specific wear is approximately $188.9 \times 10^{-7}\ mm^2/kg$. Compared with the specific wear of Ti alloy substrate, coatings fabricated in the present study exhibit much better wear resistance. It seems that dispersed carbonitride phases improved the hardness of coating as a function of its fraction and tended to reduce the rapid removal of materials by subsurface cracking and delamination.

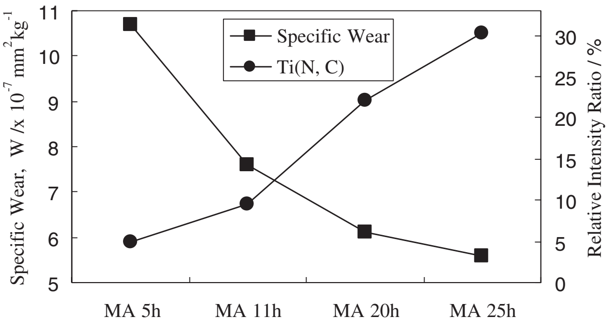

Fig. 12 Relation between specific wear of coatings prepared by attritor milled SM 200 powder batch and the relative intensity ratio of Ti(N, C) phase in each coating.

4. Conclusions

The present research has examined the preparation and characterization of ordinary attritor milled Ti-Al powders and corresponding thermal sprayed coatings fabricated by LPPS. The results of the present research can be summarized as follows:

(1) Pick-up of light elements, especially N and C, into metallic materials is intensified in ordinary attritor milling even at room temperature condition with both higher ball to powder ratio and longer milling time.

(2) By introducing the milled powder prepared by the ordinary attritor milling into thermal spraying, Ti-based, fine and homogeneously distributed carbonitride precipitates appeared preferentially in the coating. Fraction of precipitated hard phases, irrespective of heat treated powders or thermal sprayed coatings, depended strongly on the milling time of the powders.

(3) It was found that the mechanism of phase formation in thermal sprayed coating is quite different from that in the normal heat treatment. That is, the higher possibility of Al evaporation during spraying might reduce the opportunity of reaction between Ti and Al elements, especially for as milled powders in the early stage of mechanical alloying, which resulted in the higher content of Ti in those coatings. On the contrary, the higher possibility of evaporation of Al might facilitate the reaction between Ti and light elements (C, N), which leaded to the formation of Ti (N, C) phase preferentially.

(4) Due to the fraction increase of the precipitates, the mechanical properties of thermal sprayed coating were effectively improved by simply increasing the milling time of powder feedstock.

Acknowledgement

The authors would like to thank Dr. Jingguo Li of Toyohashi University of Technology for his skillful assistance in the operation of TEM analysis and helpful discussions.

REFERENCES

1) F. H. Froes, C. Suryanarayana, K. Russell and C. G. Li: Mater. Sci. Eng. **A192–193** (1995) 612–623.
2) C. Suryanarayana: Prog. Mater. Sci. **46** (2001) 1–184.
3) C. Suryanarayana, E. Ivanov and V. V. Boldyrev: Mater. Sci. Eng. **A304–306** (2001) 151–158.
4) E. Bonetti, G. Cocco, S. Enzo and G. Valdrè: Mater. Sci. Technol. **6** (1990) 1258–1262.
5) W. Guo, S. Martelli, N. Burgio, M. Magini, F. Padella, E. Paradiso and I. Soletta: J. Mater. Sci. **26** (1990) 6190–6196.
6) G. Cocco and I. Soletta: Philos. Mag. **B61** (1990) 473–486.
7) W. Guo, S. Martelli, F. Padella, M. Magini, N. Burgio, E. Paradiso and U. Franzoni: Mater. Sci. Forum **88–90** (1992) 139–146.
8) T. Itsukaichi, K. Masuyama, M. Umemoto and I. Okane: Mater. Sci. Forum **88–90** (1992) 631–638.
9) C. Suryanarayana, G. H. Chen, A. Frefer and F. H. Froes: Mater. Sci. Eng. **A158** (1992) 93–101.
10) T. Suzuki, T. Ino and M. Nagumo: Mater. Sci. Forum **88–90** (1992) 639–646.
11) J. Keskinen, A. Pogany, J. Rubin and P. Ruuskanen: Mater. Sci. Eng. **A196** (1995) 205–211.
12) L. Pawlowski: *The Science and Engineering of Thermal Spray Coating*, (John Wiley & Sons Ltd, Chichester, England, 1995).
13) I. Yuki, N. Amano, M. Uozumi, H. Inui and M. Yamaguchi: J. Jpn. Inst. Metals **58** (1994) 564–570.
14) Y. Tsunekawa, M. Okumiya, M. Okuda and M. Fukumoto: *Surface Modification Technologies VI*, (The institution of Materials, London, 1998) pp. 234–245.
15) Y. Hoshiyama, H. Miyake, K. Murakami and H. Nakajima: Mater. Sci. Eng. **A333** (2002) 92–97.
16) PDF2 plus for windows, Version 3.2.0 (Digital Data Management Corp, 2004).
17) K. Y. Wang: J. Mater. Sci. **30** (1995) 5427–5432.
18) P. Fauchais: J. Phys. D: Appl. Phys. **37** (2004) 86–108.
19) J. P. Kuang, R. A. Harding and J. Campbell: Mater. Sci. Eng. **A329** (2002) 31–37.